Three-Dimensional Tumor Margin Demarcation Using the Hybrid Tracer Indocyanine Green-^{99m}Tc-Nanocolloid: A Proof-of-Concept Study in Tongue Cancer Patients Scheduled for Sentinel Node Biopsy

Philippa Meershoek[1,2], Nynke S. van den Berg[1], Oscar R. Brouwer[1], H. Jelle Teertstra[3], Charlotte A.H. Lange[3], Renato A. Valdés-Olmos[1], Bernies van der Hiel[4], Alfons J.M. Balm[2], W. Martin C. Klop[2], and Fijs W.B. van Leeuwen[1,2]

[1]Interventional Molecular Imaging Laboratory, Department of Radiology, Leiden University Medical Center, Leiden, The Netherlands; [2]Department of Head-and-Neck Surgery, Netherlands Cancer Institute–Antoni van Leeuwenhoek Hospital, Amsterdam, The Netherlands; [3]Department of Radiology, Netherlands Cancer Institute–Antoni van Leeuwenhoek Hospital, Amsterdam, The Netherlands; and [4]Department of Nuclear Medicine, Netherlands Cancer Institute–Antoni van Leeuwenhoek Hospital, Amsterdam, The Netherlands

For radical resection of squamous cell carcinoma of the oral cavity, a tumor-free margin of at least 5 mm is required. Unfortunately, establishing in-depth margins is a surgical conundrum. Knowing that the hybrid sentinel node (SN) tracer indocyanine green (ICG)-^{99m}Tc-nanocolloid generates temporary tattoolike markings at the site of administration, we studied the ability to apply this tracer for tumor margin demarcation combined with SN biopsy. **Methods:** Nineteen patients with clinical T1–T2 oral tongue tumors received the traditional superficial 3 or 4 deposits of ICG-^{99m}Tc-nanocolloid (0.1 mL each), and in 12 patients additional deposits were placed deeply using ultrasound guidance (total of 6; 0.07 mL each). SN mapping was performed using lymphoscintigraphy and SPECT/CT. Before and directly after tumor excision, fluorescence imaging was performed to monitor the tracer deposits in the patient (fluorescent deposits were not used to guide the surgical excision). At pathologic examination, primary tumor samples were studied in detail. **Results:** The number of tracer depositions did not induce a significant difference in the number of SNs visualized (P = 0.836). Reproducible and deep tracer deposition proved to be challenging. The fluorescent nature of ICG-^{99m}Tc-nanocolloid supported in vivo and ex vivo identification of the tracer deposits surrounding the tumor. Pathologic examination indicated that in 66.7% (8/12), all fluorescence was observed within the resection margins. **Conclusion:** This study indicates that tumor margin demarcation combined with SN identification has potential but that some practical challenges need to be overcome if this technique is to mature as a surgical guidance concept. Future studies need to define whether the technology can improve the radical nature of the resections.

Key Words: tongue cancer; image guided surgery; dual-modality; sentinel node biopsy; tumor margins

J Nucl Med 2019; 60:764–769
DOI: 10.2967/jnumed.118.220202

Positive resection margins greatly affect treatment logistics and the socioeconomic status of patients with oral cavity cancer (*1*). First, the chance of local recurrence requires that the patient needs to be scheduled for a reexcision of the primary tumor, which is coupled to an increased chance of surgery-induced morbidity. Second, nonradical surgery may drive metastatic spread, requiring additional radio- or chemotherapy (*2*). To minimize the need for reexcision, tumor-free resection margins are commonly used; for oral squamous cell carcinoma, the guidelines set a desirable margin of 0.5–1 cm (*3,4*). Although such margins can often be visibly assessed on the surface of the tissue, in-depth estimation of the tumor spread is a surgical conundrum.

The potential for real-time feedback with a high spatial resolution has triggered interest in fluorescence guidance of surgery. Various fluorescence guidance procedures are already being explored for head and neck cancer. Besides being used for the identification of lymphatic drainage patterns, such as indocyanine green (ICG)-^{99m}Tc-nanocolloid (*5–8*), fluorescent tracers have also been exploited for tumor margin delineation (*9–12*). Despite the promise of fluorescence guidance, all these studies indicate that severe tissue attenuation of the signals limits its practical use to superficial regions (<1 cm) (*13,14*). This constraint to superficial guidance, unfortunately, conflicts with the desire for surgical safety margins.

Currently, ultrasound is the most routine clinically applied modality used to address the in-depth involvement of tumors in an interventional setting (*15*). This same technology is also routinely applied to mark suggestive lesions for the surgeons' convenience using, for example, guidewires, radioactive iodine seeds, or imaging tracers (*16,17*). Tattoolike tumor staining using blue dye (*18*), or radiotracers (radiooccult lesion localization) in, for example, ^{18}F-FDG–avid lesions (*16,19*), has been applied as a minimally invasive alternative to guidewires. Since these tracers partially migrate through the lymphatic system, they also support the identification of sentinel nodes (SNs) (*20*). Hence, the tracer administration may support 2 complementary clinical demands: identification of the primary tumor and identification of SNs (*21*).

Generally, for SN biopsy of oral squamous cell carcinoma, 3 or 4 tracer deposits of ICG-^{99m}Tc-nanocolloid are placed around the

Received Sep. 12, 2018; revision accepted Oct. 26, 2018.
For correspondence or reprints contact: Fijs W.B. van Leeuwen, Interventional Molecular Imaging Laboratory, Department of Radiology, Leiden University Medical Center (LUMC), Albinusdreef 2, P.O. Box 9600, Postal Zone C2-S, 2300 RC, Leiden, The Netherlands.
E-mail: f.w.b.van_leeuwen@lumc.nl
Published online Nov. 30, 2018.

tumor (*20*). We reasoned that increasing the number of deposits and including in-depth deposits placed using ultrasound guidance could help support 3-dimensional intraoperative tumor margin assessment in the tongue while preserving the tracer's ability to guide SN resections (Figs. 1A and 1B). To study this hypothesis, we compared a cohort of patients who received traditional tracer deposition with a cohort who received 2 additional deep deposits. Fluorescence imaging—in vivo, ex vivo, and in pathologic samples—was used to assess the accuracy of the margin-staining technique.

MATERIALS AND METHODS

Patients

Patient inclusion criteria were an age of 18 y or older, histologically proven squamous cell carcinoma of the oral tongue, clinical T1–T2 tumor, and a regional clinical node-negative lymph node status as defined by ultrasound or fine-needle aspiration cytology. To be included, patients also had to be scheduled for primary tumor excision with subsequent SN biopsy. Pregnant or breast-feeding women and patients with a known allergy to iodine were excluded from participation in the study.

The study protocol was approved by the review board of the institute (study protocol NL26699.031.09). Patients were included after providing written informed consent.

Tracer Preparation

As reported previously (*20*), ICG-^{99m}Tc-nanocolloid was produced in line with good manufacturing practice and under the supervision of the institution's pharmacist.

Tracer Injection

All patients received local anesthesia in the form of a 10% xylocaine spray 10 min before tracer administration. Subsequently, using a Hitachi EUB-900 ultrasound system with an additional Hitachi transducer (hockey-stick model EUP-054J), a radiologist placed the needle, after which a nuclear medicine physician injected the tracer deposit. A dose of approximately 80 MBq of ICG-^{99m}Tc-nanocolloid was injected in a maximum of 6 deposits using a total injection volume of 0.4 mL. Attempts were made to deposit tracer approximately 1–2 mm from the border of the tongue tumor. Superficial deposits were used to mark the lateral (or caudal), medial (or cranial), posterior, and anterior borders of the tumor. In 1 cohort, 2 additional deeply placed injections were given under ultrasound guidance to demarcate the primary tumor in 3 dimensions (Fig. 1).

Preoperative SN Mapping

Preoperative imaging was performed as previously described (*20*). For each patient, the number and anatomic locations of the SNs were scored.

Surgical Procedure

SN Biopsy Procedure. Radioguided and fluorescence-guided SN biopsy was performed as previously described (*20*).

Tongue Tumor Excision. Preceding excision of the primary tumor, near-infrared fluorescence imaging of the injection site (PDE; Hamamatsu Photonics K.K.) was performed to evaluate whether the injected tracer deposits could be visualized. Thereafter, the primary tumor was surgically excised according to standard procedures (optical free margin minimally 1.0 cm wide). In the patients who received 3-dimensional tumor demarcation, after surgical excision, the wound bed and the freshly excised tongue tumor specimen were examined for fluorescence hot spots. Because of ethical considerations, excision of the primary tumor was performed with the surgeon masked to the fluorescence findings. As such, we were able to ensure that the study did not cause a deviation in the standard of care.

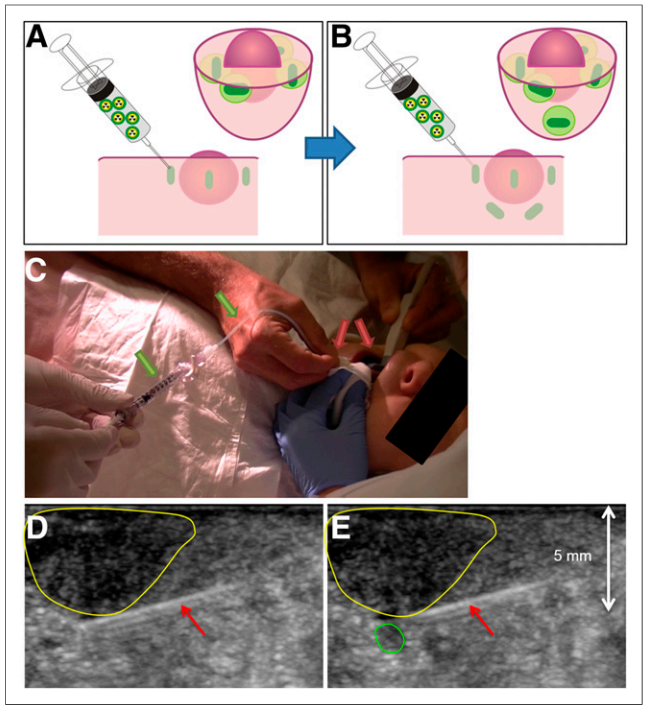

FIGURE 1. Injection method. (A) Standard SN procedure consists of 3–4 superficial injections surrounding tumor. (B) In this study, 12 patients received additional injections, placed deep behind tumor using ultrasound guidance. (C) Radiologist inserts injection needle under ultrasound guidance (red arrows). Nuclear physician then injects ICG-^{99m}Tc-nanocolloid via syringe-tubing system (green arrows). (D) Radiologist keeps needle (red arrows) 1–2 mm next to tumor border (yellow area) while nuclear physician injects tracer. (E) Deposit of ICG-^{99m}Tc-nanocolloid can be visualized on ultrasound (green area).

Pathology

Primary Tumor Samples. The excised tissue was formalin-fixed, after which it was cut into 5.0-mm slices and paraffin-embedded. Hematoxylin and eosin (H&E) staining was performed on each section. The pathologist determined the location and extent of the primary tumor and used indelible ink to mark the location on the slides.

Formalin-fixed paraffin-embedded tongue samples were evaluated ex vivo for the location of the hybrid tracer in the specimen. Each section was imaged on an IVIS-200 system (ICG filter settings: excitation, 710–760 nm; emission, 810–875 nm [Xenogen Corp.]). The location of the fluorescent signal was then compared with the location of the tumor margins. Using an overlay of the IVIS images and H&E-stained slides, we measured the distance from the center of the fluorescence signal to the closest tumor border using RulerSwift, version 1.0 (by Zhi Li, available in the Mac App Store).

SN Samples. Excised SNs were formalin-fixed, bisected into 5.0-mm sections, paraffin-embedded, and cut at a minimum of 6 levels at 50- to 150-μm intervals. Histopathologic evaluation included staining with H&E and anticytokeratin (CAM5.2; Becton Dickinson).

RESULTS

The study population consisted of 31 patients, of whom 12 were in the tumor demarcation group and 19 in the control group

(Supplemental Table 1; supplemental materials are available at http://jnm.snmjournals.org). Their average age was 61 ± 11 and 59 ± 10 y, respectively.

Injection Procedure

In all patients, ICG-^{99m}Tc-nanocolloid could be administered without complications. Although injection of the hybrid tracer deposits surrounding the visual superficial borders of the tumor was relatively straightforward, identification of the deep edges of the tumor using ultrasound was considerably more challenging, especially in patients with deeply infiltrating tumors physically restricting the intraoral space available for placement of the ultrasound probe and syringe. Despite application of xylocaine spray as a local anesthetic, patients considered the deeper injections to be painful. Involuntary movements of the tongue further complicated tracer deposition. The set-up used also made it difficult to administer the tracer in equal volumes and at equal pressure. Hence, we observed variations in the size of the deposits.

SN Identification

Preoperative SN imaging and identification rates for both groups are provided in Supplemental Figure 1 and Table 1, respectively. Interestingly, these data indicate that variations in the number and location of the tracer deposits in the tongue did not affect SN identification.

Surgical Procedure

The number of SNs that were excised did not significantly differ between the 2 groups (Table 1).

Before surgical excision of the primary tumor, the superficial ICG-^{99m}Tc-nanocolloid deposits could be visualized with fluorescence imaging (Fig. 2). Only in 1 patient the use of SPECT/CT allowed separate visualization of 6 tracer deposits (Supplemental Fig. 1). The excision was performed with the surgeon masked to these findings. After excision of the primary tumor, the presence of fluorescence in the surgical wound bed could be imaged (Fig. 2).

Ex Vivo Tissue Analysis of Samples from the 6-Deposit Patient Cohort

Tracer deposits in excised tumor specimens could clearly be visualized with fluorescence imaging (Fig. 2). They could also be detected in embedded pathologic specimens. Figure 3 presents an overlay of such fluorescence images with the matching H&E-stained slides. Overall, the median distance between the core of the tracer deposit and the tumor border was 2.8 mm (mean, 3.5 mm; range, 0.2–15.1 mm; Table 2). In 4 patients (33.3%), the center of 1 tracer deposition overlapped with the tumor tissue, indicating inaccurate ultrasound-guided tracer deposition. The center of these intratumoral tracer deposits was, on average, 1.7 mm inside the tumor border (median, 1.2 mm; range, 0.2–4.2 mm; Table 2). In the other 8 patients (66.7%), the center of the fluorescent deposits

TABLE 1
Preoperative, Intraoperative, and Pathologic Findings

Parameter	Tumor tattooing	Standard SN procedure	*P*
Mean administered dose (MBq) ± SD	100.0 ± 34.8 (median, 95.9)	78.7 ± 7.3 (median, 79.0)	0.059
Preoperative SN-related hot spots (*n*)			
Lymphoscintigraphy	34 (median per patient, 2)	50 (median per patient, 2)	0.674
SPECT/CT	34 (median per patient, 2)	52 (median per patient, 3)	0.836
Mean intraoperative SN results			
Fluorescent, in vivo	4.0 (median, 3)	2.7 (median, 2.5)	0.192
Fluorescent, ex vivo	3.8 (median, 3.5)	3.2 (median, 3)	0.365
Radioactive, in vivo	2.9 (median, 3)	2.7 (median, 2.5)	0.745
Radioactive, ex vivo	4.0 (median, 4)	3.0 (median, 3)	0.159
Total excised SNs (*n*)	54 (mean, 4.5; median, 4)	60 (mean, 3.2; median, 3)	0.090
Total excised non-SNs (*n*)	11 (mean, 0.9; median, 0.5)	9 (mean, 0.5; median, 0)	0.215
Total excised nodes (*n*)	65	69	
Pathology (*n*)			
SNs	84	83	0.072
Non-SNs	32	7	0.306
Total nodes	116	90	0.060
Tumor-positive SNs	5 (in 3 patients)	5 (in 4 patients)	
Tumor-positive non-SNs	1* (in 1 patient)	0	
Tumor-positive nodes	6 (in 3 patients)	5 (in 4 patients)	
Resection status (*n*)			
R0	11 (91.7%)	19 (100.0%)	
R1	1 (8.3%)	0	

*In this patient, 1 SN was also found tumor-positive.

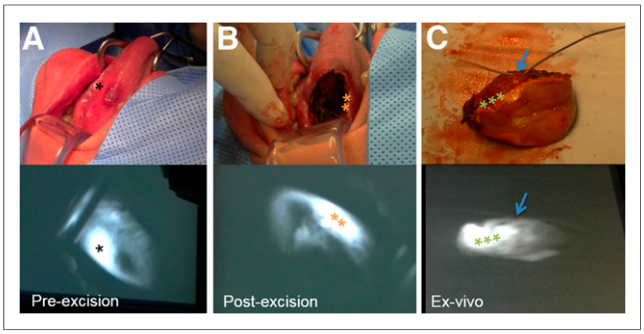

FIGURE 2. White light (top) and fluorescence (bottom) imaging during procedure. (A) Preexcision image of tumor. (B) Postexcision image of same tumor. (C) Tumor tissue ex vivo. Stitch in excised tissue marks anterior side (arrow). *Tracer deposit. **Remaining fluorescence signal. ***Tracer deposit surrounding tumor.

was outside the tumor border, but fluorescence was detected within the margin. Only 2 deposits (2/72; 2.8%) in 2 patients were located outside the 10-mm resection margin.

Pathology

Table 1 shows the preoperative, intraoperative, and pathologic SN findings and resection statuses. Table 2 shows the fluorescence findings in the primary tumor specimens.

One patient (8.3%) of the tumor demarcation group had an R1 resection. This patient had 3 tumor-positive SNs at pathology. Analysis revealed that the tracer deposits were accurately placed outside the tumor border (0.2–2.2 mm) and inside the resection

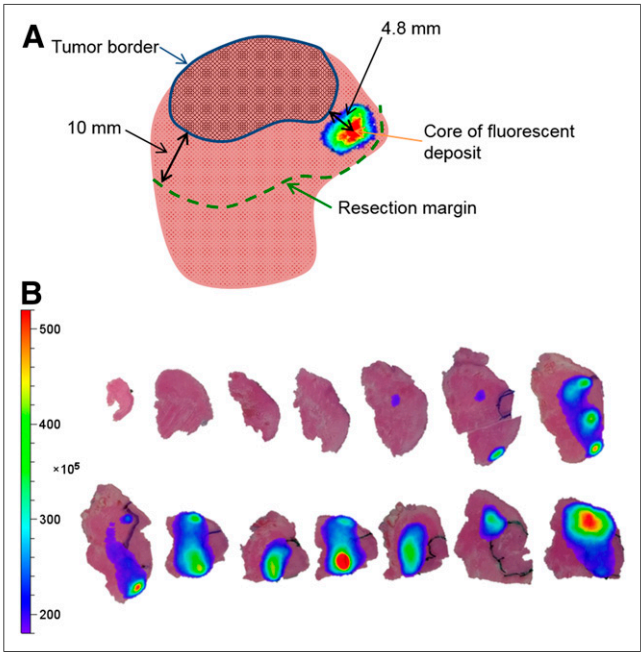

FIGURE 3. Schematic overview of pathologic analysis. (A) Tumor has been marked on H&E-stained slides with indelible ink. Overlay of fluorescence signal is projected onto original image. Distance has been measured between core of fluorescent spots and tumor border as drawn on slides. (B) H&E-stained slides from patient in tumor demarcation group with overlay of fluorescence signal. Fluorescent deposits in excised tumor tissue can be visualized, and distance between fluorescent cores and tumor border was measured.

TABLE 2
Fluorescence Findings in Excised Tissue

Parameter	Data
Fluorescent spots on tissue section with tumor tissue (*n*)	62
Fluorescence signal outside tumor tissue (*n*)	58/62 (93.5%)
Fluorescence signal within 10-mm margin	56/58 (96.6%)
Fluorescence signal outside 10-mm margin	2/58 (3.4%)
Fluorescence signal inside tumor tissue (*n*)	4/62 (6.5%)
Patients with all fluorescent spots 0–10 mm outside tumor border (*n*)	8/12 (66.7%)
Patients with fluorescent spot inside tumor (*n*)	4/12 (33.3%)
Distance from tumor border to fluorescence signal outside tumor (mm)	
Median	2.8
Mean	3.2
Range	0.2–10.2 (IQR, 1.3–4.3)
Distance from tumor border to fluorescence signal inside tumor (mm)	
Median	1.2
Mean	1.7
Range	0.2–4.2

IQR = interquartile range.

margin. Perhaps using fluorescence to guide the primary tumor excision could have made a difference in this case.

DISCUSSION

Our findings indicate that intraoperative visualization of deeply placed deposits of ICG-^{99m}Tc-nanocolloid is possible using fluorescence imaging. Further, the placement of 2 additional deep tracer deposits did not negatively influence the lymphatic drainage pattern. This result suggests that the tumor margin demarcation procedure can be integrated in SN mapping.

Today, fluorescence guidance is considered a popular research tool for refining surgical margins. For this application, increasing numbers of tumor-specific fluorescent tracers are being developed and evaluated in clinical trials (*22–24*). Although all these examples have proven to be capable of superficially depicting fluorescence accumulation in tumors, none has yet demonstrated the ability to define surgical safety margins in vivo. For margin assessment, the fluorescence signal intensity should be directly related to the distance to the edge of the tumor. Other than with radiologic modalities (*25*), deep margin assessment by fluorescence is currently limited by 3 factors: the effect of signal attenuation on the depth reached by today's fluorescence imaging technologies (<1 cm) (*13*), the influence of tracer concentration on

intraoperative tracer detectability (*26*), and heterogeneous tracer uptake in tumors (*27*). Although heterogeneous tracer distribution did not limit our approach, our findings confirm that detection of deep fluorescence signals was limited and influenced by the amount of tracer in a deposit. As deep margin assessment represents a true unmet clinical need, the shortcomings of fluorescence imaging indicate that multiplexing with radiologic modalities is required by using, for example, dual-modality tracers such as ICG-^{99m}Tc-nanocolloid.

In the field of radiology, image-guided needle placement using, for example, ultrasound, fluoroscopy, CT, or MRI is a standard and well-validated technique for biopsy, tumor marking, and tumor ablation (*28,29*). For applications in which morphologic features do not provide sufficient guidance, nuclear imaging technologies are increasingly being used (*19*). Moreover, the accuracy of needle placement has been improved substantially through the use of augmented-reality and virtual-reality navigation technologies (*30*). From a practical and patient perspective, it makes sense to exploit this clinical expertise to help advance margin identification during surgical resections. In the present study, needle placement and the refinement of the tracer deposit size was facilitated by the fact that a radiologist placed the needle and a nuclear medicine physician injected the radioactive tracer. Practical challenges were encountered predominantly during the deep tumor demarcation. These challenges stemmed from the limited physical space available for needle and ultrasound placement, involuntary movement of the tongue, and difficulty in controlling the size of the tracer deposit. Since the 2 additional deposits did not influence the SN drainage, 2 deep deposits of ICG-nanocolloid (no ^{99m}Tc) could theoretically be placed when the patient is fully sedated before surgery. This step would also solve accessibility and involuntary movement and would reduce the discomfort experienced by patients. Theoretically, the margin size can be refined by optimizing the injection volume (e.g., through microinjectors), the pressure applied during injection, or the particle size of the tracer (*31*).

Interestingly, the number and location of tracer deposits did not yield a significant difference in SN visualization. This observation is in line with the reported lymphatic drainage patterns of the tongue (*32*), which indicate that the lymphatic vessels of the tongue drain mostly to the submandibular (anterior and lateral vessels) and subdigastric (lateral and posterior vessels) lymph nodes.

The generic applicability of the tattoolike approach presented here and the fact that the hybrid SN tracer ICG-^{99m}Tc-nanocolloid is increasingly being used in clinics across the globe (*20,33–35*) provide a strong stepping stone to further dissemination. This use is supported by increasing awareness of the value of the SN concept for head and neck cancers.

CONCLUSION

Intraoperative visualization of ICG-^{99m}Tc-nanocolloid tracer deposits in the margins of tongue tumors proved to be technically feasible. In this setting, the administration of 2 extra deeply placed extra tracer depositions did not lead to a difference in the number of preoperatively identified SNs. By demonstrating the technical feasibility of the hybrid tumor-margin tattoo concept, we have opened the possibility of exploring further refinements of the presented concept and its use to guide primary tumor excisions.

DISCLOSURE

This research was partially supported by a STW-VIDI grant from the Netherlands Organization for Scientific Research (grant STW BGT11272) and a grant from the European Research Council under the European Union's Seventh Framework Program (FP7/2007-2013) (grant 2012-306890). No other potential conflict of interest relevant to this article was reported.

REFERENCES

1. Binahmed A, Nason RW, Abdoh AA. The clinical significance of the positive surgical margin in oral cancer. *Oral Oncol.* 2007;43:780–784.
2. Smits RW, Koljenovic S, Hardillo JA, et al. Resection margins in oral cancer surgery: room for improvement. *Head Neck.* 2016;38(suppl 1):E2197–E2203.
3. Ravi SB, Annavajjula S. Surgical margins and its evaluation in oral cancer: a review. *J Clin Diagn Res.* 2014;8:ZE01–ZE05.
4. Yamada S, Kurita H, Shimane T, et al. Estimation of the width of free margin with a significant impact on local recurrence in surgical resection of oral squamous cell carcinoma. *Int J Oral Maxillofac Surg.* 2016;45:147–152.
5. Hirono S, Tani M, Kawai M, et al. Identification of the lymphatic drainage pathways from the pancreatic head guided by indocyanine green fluorescence imaging during pancreaticoduodenectomy. *Dig Surg.* 2012;29:132–139.
6. Handgraaf HJ, Boogerd LS, Verbeek FP, et al. Intraoperative fluorescence imaging to localize tumors and sentinel lymph nodes in rectal cancer. *Minim Invasive Ther Allied Technol.* 2016;25:48–53.
7. Ayestaray B, Bekara F. Fluorescein sodium fluorescence microscope-integrated lymphangiography for lymphatic supermicrosurgery. *Microsurgery.* 2015;35:407–410.
8. KleinJan GH, van Werkhoven E, van den Berg NS, et al. The best of both worlds: a hybrid approach for optimal pre- and intraoperative identification of sentinel lymph nodes. *Eur J Nucl Med Mol Imaging.* 2018;45:1915–1925.
9. de Boer E, Harlaar NJ, Taruttis A, et al. Optical innovations in surgery. *Br J Surg.* 2015;102:e56–e72.
10. KleinJan GH, van den Berg NS, de Jong J, et al. Multimodal hybrid imaging agents for sentinel node mapping as a means to (re)connect nuclear medicine to advances made in robot-assisted surgery. *Eur J Nucl Med Mol Imaging.* 2016;43:1278–1287.
11. Inoue T, Endo T, Nagamatsu K, Watanabe M, Tominaga T. 5-aminolevulinic acid fluorescence-guided resection of intramedullary ependymoma: report of 9 cases. *Neurosurgery.* 2013;72(suppl):ons159–168.
12. Warram JM, de Boer E, Korb M, et al. Fluorescence-guided resection of experimental malignant glioma using cetuximab-IRDye 800CW. *Br J Neurosurg.* 2015;29:850–858.
13. van Leeuwen FW, Valdes-Olmos R, Buckle T, Vidal-Sicart S. Hybrid surgical guidance based on the integration of radionuclear and optical technologies. *Br J Radiol.* 2016;89:20150797.
14. Chin PT, Beekman CA, Buckle T, Josephson L, van Leeuwen FW. Multispectral visualization of surgical safety-margins using fluorescent marker seeds. *Am J Nucl Med Mol Imaging.* 2012;2:151–162.
15. Wagner JM, Conrad RD, Cannon TY, Alleman AM. Ultrasound-guided transcutaneous needle biopsy of the base of the tongue and floor of the mouth from a submental approach. *J Ultrasound Med.* 2016;35:1009–1013.
16. Sajid MS, Parampalli U, Haider Z, Bonomi R. Comparison of radioguided occult lesion localization (ROLL) and wire localization for non-palpable breast cancers: a meta-analysis. *J Surg Oncol.* 2012;105:852–858.
17. Luiten JD, Beek MA, Voogd AC, Gobardhan PD, Luiten EJ. Iodine seed- versus wire-guided localization in breast-conserving surgery for non-palpable ductal carcinoma in situ. *Br J Surg.* 2015;102:1665–1669.
18. Ahn D, Ho Sohn J, Park J, Eun Lee J. Ultrasound-guided intratumoral indigo carmine injection for intraoperative, surgeon-performed tumor localization. *Head Neck.* 2014;36:1317–1323.
19. KleinJan GH, Brouwer OR, Matheron HM, et al. Hybrid radioguided occult lesion localization (hybrid ROLL) of ^{18}F-FDG-avid lesions using the hybrid tracer indocyanine green-^{99m}Tc-nanocolloid. *Rev Esp Med Nucl Imagen Mol.* 2016;35:292–297.
20. van den Berg NS, Brouwer OR, Klop WM, et al. Concomitant radio- and fluorescence-guided sentinel lymph node biopsy in squamous cell carcinoma of the oral cavity using ICG-^{99m}Tc-nanocolloid. *Eur J Nucl Med Mol Imaging.* 2012;39:1128–1136.

21. Ahmed M, Douek M. Sentinel node and occult lesion localization (SNOLL): a systematic review. *Breast.* 2013;22:1034–1040.
22. van Dam GM, Themelis G, Crane LM, et al. Intraoperative tumor-specific fluorescence imaging in ovarian cancer by folate receptor-alpha targeting: first in-human results. *Nat Med.* 2011;17:1315–1319.
23. Burggraaf J, Kamerling IM, Gordon PB, et al. Detection of colorectal polyps in humans using an intravenously administered fluorescent peptide targeted against c-Met. *Nat Med.* 2015;21:955–961.
24. Rosenthal EL, Warram JM, de Boer E, et al. Safety and tumor specificity of cetuximab-IRDye800 for surgical navigation in head and neck cancer. *Clin Cancer Res.* 2015;21:3658–3666.
25. Maurer T, Robu S, Schottelius M, et al. ^{99m}Technetium-based prostate-specific membrane antigen-radioguided surgery in recurrent prostate cancer. *Eur Urol.* April 3, 2018 [Epub ahead of print].
26. KleinJan GH, Bunschoten A, van den Berg NS, et al. Fluorescence guided surgery and tracer-dose, fact or fiction? *Eur J Nucl Med Mol Imaging.* 2016;43: 1857–1867.
27. Beer AJ, Grosu AL, Carlsen J, et al. [^{18}F]galacto-RGD positron emission tomography for imaging of alphavbeta3 expression on the neovasculature in patients with squamous cell carcinoma of the head and neck. *Clin Cancer Res.* 2007;13: 6610–6616.
28. Gervais DA, Sabharwal T. *Interventional Radiology Procedures in Biopsy and Drainage.* New York, NY: Springer; 2011;6–20.
29. Clark T, Sabharwal T. *Interventional Radiology Techniques in Ablation.* New York, NY: Springer; 2013;120–122.
30. van Oosterom MN, van der Poel HG, Navab N, van de Velde CJH, van Leeuwen FWB. Computer-assisted surgery: virtual- and augmented-reality displays for navigation during urological interventions. *Curr Opin Urol.* 2018;28: 205–213.
31. Van Den Berg NS, Buckle T, Kleinjan GI, et al. Hybrid tracers for sentinel node biopsy. *Q J Nucl Med Mol Imaging.* 2014;58:193–206.
32. Pan W-R, le Roux CM, Levy SM, Briggs CA. Lymphatic drainage of the tongue and the soft palate. *Eur J Plast Surg.* 2010;33:251–257.
33. Brouwer OR, van den Berg NS, Matheron HM, et al. A hybrid radioactive and fluorescent tracer for sentinel node biopsy in penile carcinoma as a potential replacement for blue dye. *Eur Urol.* 2014;65:600–609.
34. Christensen A, Juhl K, Charabi B, et al. Feasibility of real-time near-infrared fluorescence tracer imaging in sentinel node biopsy for oral cavity cancer patients. *Ann Surg Oncol.* 2016;23:565–572.
35. Paredes P, Vidal-Sicart S, Campos F, et al. Role of ICG-^{99m}Tc-nanocolloid for sentinel lymph node detection in cervical cancer: a pilot study. *Eur J Nucl Med Mol Imaging.* 2017;44:1853–1861.